iScience

CellPress
OPEN ACCESS

Article

Evolution of ion transporter Na^+/K^+-ATPase expression in the osmoregulatory maxillary glands of an invasive copepod

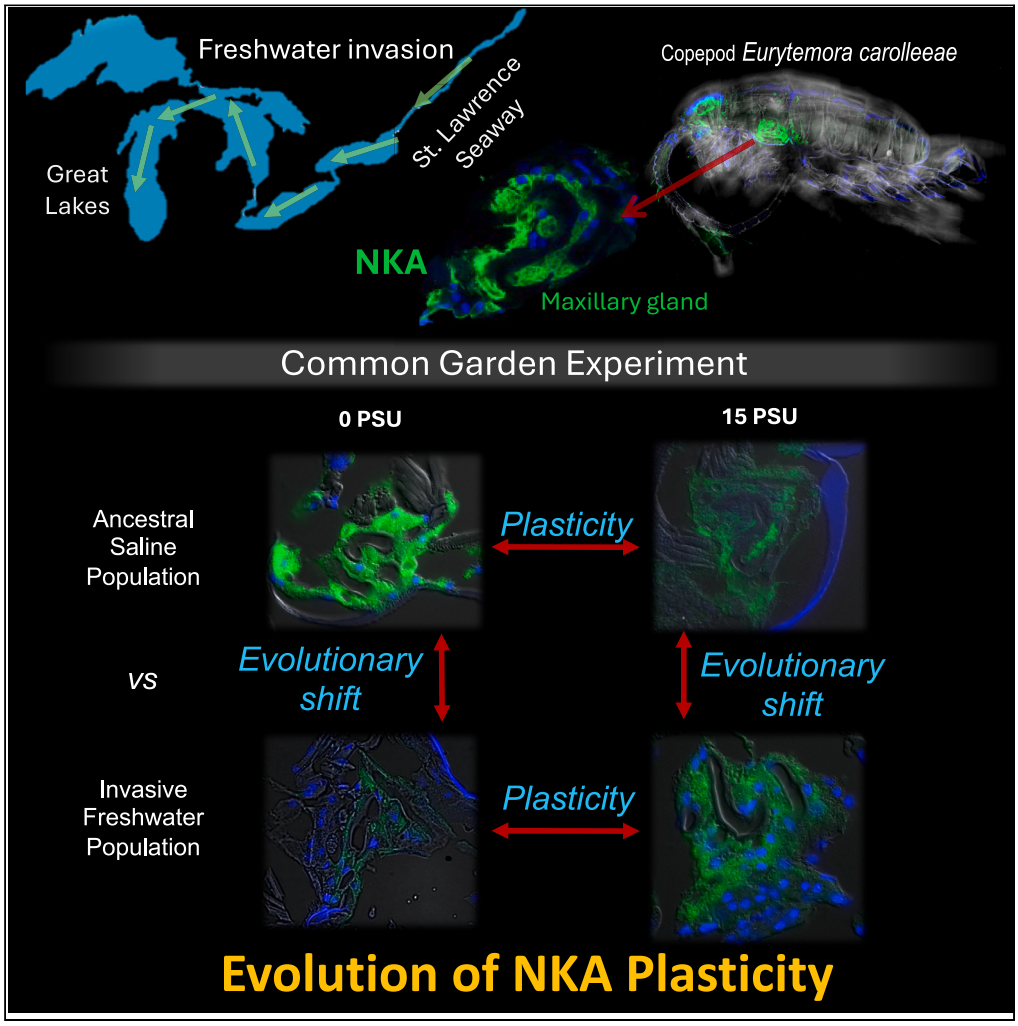

Teresa E. Popp, Sophie Hermet, Jacob Fredette-Roman, ..., Guy Charmantier, Carol Eunmi Lee, Catherine Lorin-Nebel

carollee@wisc.edu (C.E.L.)
catherine.lorin@umontpellier.fr (C.L.-N.)

Highlights

NKA expression level in maxillary glands (MG) evolves from ancestral to invading populations

Plasticity in MG NKA expression level evolves toward canalization in the freshwater population

Saline population shows higher MG NKA expression level at 0 PSU than the freshwater population

Popp et al., iScience 27, 110278
July 19, 2024
https://doi.org/10.1016/j.isci.2024.110278

iScience

CellPress
OPEN ACCESS

Article

Evolution of ion transporter Na^+/K^+-ATPase expression in the osmoregulatory maxillary glands of an invasive copepod

Teresa E. Popp,[1,2] Sophie Hermet,[1] Jacob Fredette-Roman,[2] Emma McKeel,[2,3] William Zozaya,[1] Corentin Baumlin,[1] Guy Charmantier,[1] Carol Eunmi Lee,[1,2,*] and Catherine Lorin-Nebel[1,4,*]

SUMMARY

While many freshwater invaders originate from saline habitats, the physiological mechanisms involved are poorly understood. We investigated the evolution of ion transporter Na^+/K^+-ATPase (NKA) protein expression between ancestral saline and freshwater invading populations of the copepod *Eurytemora carolleae* (Atlantic clade of the *E. affinis* complex). We compared *in situ* NKA expression between populations under common-garden conditions at three salinities in the maxillary glands. We found the evolution of reduced NKA expression in the freshwater population under freshwater conditions and reduced plasticity (canalization) across salinities, relative to the saline population. Our results support the hypothesis that maxillary glands are involved in ion reabsorption from excretory fluids at low-salinity conditions in the saline population. However, mechanisms of freshwater adaptation, such as increased ion uptake from the environment, might reduce the need for ion reabsorption in the freshwater population. These patterns of ion transporter expression contribute insights into the evolution of ionic regulation during habitat change.

INTRODUCTION

Human-induced destructive impacts in the current Anthropocene, such as climate change, biological invasions, and habitat destruction, are causing natural populations to experience dramatic shifts in environmental conditions.[1–3] Such rapid and destructive impacts are exposing many populations to conditions beyond their natural physiological niches. For instance, climate change is causing the rapid freshening of high latitude coastal seas[4–10] and increases in salinities in many low latitude environments, such as the Mediterranean Sea.[11–13] Populations are also experiencing rapid salinity changes during biological invasions. Most notably, freshwater habitats are now dominated by invaders from more saline habitats.[14,15] Some notable examples include the invasions of the North American Great Lakes by brackishwater populations from the Black and Caspian Seas, likely through ballast water transport and dumping,[16–20] such as the fishhook water flea *Cercopagis pengoi*[18], the zebra mussel *Dreissena polymorpha*, and the quagga mussel *Dreissena bugensis*.[21,22] Such invasive populations that cross habitat boundaries provide valuable models for studying evolutionary responses to rapid habitat change, allowing the study of rapid physiological changes on contemporary time scales.[23]

The salinity boundary of 5 PSU (practical salinity unit ≈ parts per thousand salinity) represents a biogeographical barrier that many animal populations cannot overcome.[24] Rapid changes in habitat salinity, especially across this salinity boundary, can threaten the survival of populations, given the serious challenges that novel ionic and osmotic conditions pose for organisms to maintain internal homeostasis.[14,25–27] Populations facing rapid salinity changes can survive through alternative strategies, such as migrating to avoid the changes, acclimating through phenotypic plasticity, and/or adapting through natural selection.[13] In many cases, evolutionary processes play crucial roles in determining the ability of populations to survive under changing environmental conditions.[28,29]

Acclimating or adapting to novel salinities would involve osmotic and ionic regulatory mechanisms to maintain the balance of ions and water within an organism (i.e., hydromineral homeostasis).[26] One physiological mechanism involves minimizing ionic losses, either through the reabsorption of ions by excretory organs (via the action of ion transporters) or by reducing the permeability of the integument.[27,30] Another strategy involves increasing ion uptake from the surrounding environment by increasing the activity and/or expression of ion transporters, typically embedded within specialized osmoregulatory organs.[25] Extensive research has been conducted on mechanisms of ionic regulation in fish, some decapod crustaceans, and model insects,[25,31,32] particularly focusing on their gills, digestive tract, and excretory organs (e.g., kidneys, antennal glands, and Malpighian tubules).[33,34] For example, brachyuran crabs typically tolerate freshwater environments

[1]MARBEC, Univ Montpellier, CNRS, IRD, Ifremer, Montpellier, France
[2]Department of Integrative Biology, University of Wisconsin, 430 Lincoln Drive, Madison, WI 53706, USA
[3]Present address: School of Freshwater Sciences, University of Wisconsin, 600 E. Greenfield Avenue, Milwaukee, WI 53204
[4]Lead contact
*Correspondence: carollee@wisc.edu (C.E.L.), catherine.lorin@umontpellier.fr (C.L.-N.)
https://doi.org/10.1016/j.isci.2024.110278

by employing specialized ion transport mechanisms in their gills and antennal glands to maintain osmotic balance, whereas anomuran crabs rely more on behavioral adaptations and unique gill structures to manage osmotic challenges.[35,36] Comparatively less attention has been focused on hyperosmoregulating non-model invertebrates,[34,37] especially those lacking these specialized organs. Thus, the current study focuses on investigating osmoregulation in copepods, which lack traditional gills or antennal glands, highlighting the understudied nature of copepods' osmoregulatory organs and their potential role in freshwater tolerance.

The copepod *Eurytemora affinis* species complex is native to coastal waters in the Northern Hemisphere, including estuaries and salt marshes in North America, Europe, and Asia, where it is a dominant constituent of zooplankton communities.[38–40] In many saline bays and estuaries, populations of the *E. affinis* complex support some of the world's most important fisheries, including herring, anchovy, larval salmon, and smelt.[41,42] Furthermore, the *E. affinis* complex has served as a model system for evolutionary and ecological studies due to its broad distribution and ability to adapt to rapid environmental change.[23,43–49] Notably, estuarine and saltmarsh populations of *E. affinis* complex have colonized freshwater habitats independently across the Northern Hemisphere over the past ~80 years.[38] These recent freshwater invasions allow us to study physiological mechanisms of adaption and acclimation in response to salinity decline and gain insights into responses to future alterations in habitat salinity induced by climate change.

The rapid freshwater invasions by *E. affinis* complex populations are remarkable, given that copepods are crustaceans that do not possess gills. Our previous investigations localized ion regulatory sites in atypical anatomical structures in these copepods. Specifically, we localized ion transporter expression in the swimming legs (the "Crusalis organs"), which are likely involved in ion uptake from the environment, and in the maxillary glands, where ion reuptake from the urine might take place.[37,50] Notably, ionocytes, which are specialized cells involved in ion transport, were localized in both the maxillary glands and within the swimming legs.[51,52] Furthermore, the primary active ion transporters Na^+/K^+-ATPase (NKA) and V-type H^+ ATPase (VHA) were immunolocalized within ionocytes in these glands and tissues.[51,52] These findings on the relatively unexplored organs proposed for iono-regulation in *E. affinis* complex populations suggest the importance of alternative ion uptake and reuptake pathways in the absence of other well-studied osmoregulatory organs, such as insect Malpighian tubules or crustacean gills and antennal glands.

In addition, our previous research into mechanisms of adaptation into freshwater habitats by *E. affinis* complex populations have identified ion transporters as the major targets of natural selection during salinity change.[49,53–57] For instance, key ion transporters repeatedly showed genomic signatures of natural selection during independent saline to freshwater invasions in wild populations[53] and during salinity decline in replicate laboratory selection lines.[49,53] In addition, many of the same ion transporters showed evolutionary shifts in gene expression between saline and freshwater populations.[55] The ion transporters that were repeatedly the targets of selection during salinity change in our prior studies include paralogs of the Na^+/H^+ antiporter (*NHA*), Na^+/K^+-ATPase (*NKA*) alpha subunit, carbonic anhydrase (*CA*), and several subunits of V-type ATPase (*VHA*). Given our previous results, we were interested in exploring *in situ* evolutionary shifts of these specific ion transporters.

Thus, this study explores the evolution of ion regulatory function from saline to freshwater habitats, focusing on the poorly understood maxillary glands of *E. carolleeae* (Atlantic clade of the *E. affinis* complex). Our study focuses on ancestral saline populations in the St. Lawrence estuary and freshwater populations that have colonized the Great Lakes of North America 65 years ago[39,58] (Figure 1). The specific goals of this study were to explore (1) evolutionary shifts in patterns of localization and expression of NKA in the maxillary glands between ancestral saline and recent freshwater invading populations, (2) acclimatory changes in NKA localization and expression across three salinities (0, 5, and 15 PSU) for each population, and (3) the evolution of plasticity (population x salinity, i.e., G x E) between the saline and freshwater populations.

We disentangled the effects of evolution versus acclimation by applying a classical "common garden" approach[59,60] to determine acclimatory and heritable shifts between the saline and freshwater populations at three treatment salinities (0, 5 and 15 PSU). In these experiments, populations are first reared under "common garden" conditions to remove acclimatory effects from their native habitat before being transferred to their treatment salinities. Then the differences that remain between the populations are heritable, genetically based differences that reveal the extent to which the populations have evolved before versus after the invasion event.

We hypothesized that the maxillary glands serve as an essential component of the copepod ion regulatory system, specifically by reabsorbing ions from urine and then transporting the ions back to the hemolymph at low salinities. Crustacean maxillary glands have been hypothesized to serve as excretory organs[50,61] involved in urine production[62–64] based on morphological similarities (i.e., tubular structure and podocyte ultrastructure) with antennal glands of malacostracan crustaceans[37,65–67] and nephrons in vertebrate kidneys.[37,50] While the maxillary glands remain inadequately described, they consist of three main components: (1) the coelomic sac, where the initial filtration of hemolymph takes place, (2) the tubules, which are hypothesized to the be site of ion reabsorption, water exchange, and secretion of waste, and (3) the terminal excretory duct lined with a cuticle that opens at the base of the maxilla.[50] The tubules are characterized by the presence of apical microvilli and a complex and well-developed system of basolateral membrane infoldings, along with many mitochondria.[37,52] This morphology and ultrastructure are commonly associated with high ion transport activity and the production of dilute urine in freshwater organisms,[25,33,37,67] suggesting the potential role of the maxillary glands in ionic and hydric regulation.

If the maxillary glands do serve the function of reabsorbing ions from primary urine to reduce ionic losses, it is quite likely that these glands play important roles in adapting and acclimating to low salinity conditions. In such a scenario, we would expect that maxillary gland functions would evolve between saline and freshwater populations of the *E. affinis* complex. Thus, we predicted that NKA expression in the maxillary glands would be higher in the freshwater population relative to its saline ancestor, particularly under freshwater conditions (0 PSU), as an evolved mechanism to retain ions through ion reabsorption under low salinity conditions.

This study represents a pioneering endeavor to explore evolutionary shifts in the *in situ* expression of ion transport proteins for any organism. Additionally, this study contributes novel insights into the functions of the poorly studied crustacean maxillary glands and their role in

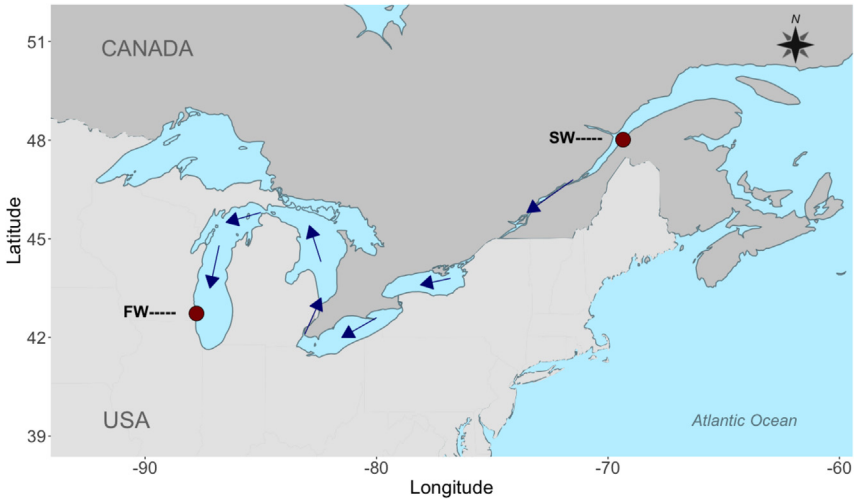

Figure 1. Pathway of freshwater invasion

(s) by populations of *E. carolleeae* (Atlantic clade of the *Eurytemora affinis complex*) from the St. Lawrence estuary into the North American Great Lakes. Arrows show the pathway of the invasion from brackish water into the freshwater lakes. Red dots indicate the locations of the saline (SW) and freshwater (FW) populations used in this study. The saline population at Baie de L'Isle Verte experiences seasonally fluctuating salinities from 5 to 40 PSU, whereas the freshwater population in Lake Michigan resides in a relatively constant salinity of 0 PSU (conductivity of ~300 μS/cm).

salinity adaptation and acclimation. This research greatly contributes to the development of mechanistic models of ion uptake in different salinity environments and the evolution of ion uptake mechanisms between populations adapted to different environments. The insights gained here are applicable for determining the physiological and evolutionary mechanisms that enable many other brackish water species to survive rapid salinity decline during freshwater invasions.[14,15,68] Moreover, these mechanisms are also relevant for high latitude coastal populations that are experiencing the freshening of their habitats due to climate change. Further exploration of ion regulatory mechanisms in hyperosmoregulating invertebrates could provide valuable new insights into the adaptive strategies that are favored by natural selection in populations that are currently facing rapid environmental salinity change.

RESULTS

To distinguish between acclimatory versus evolutionary shifts in NKA immunolocalization and expression, we performed a common garden experiment using saline and freshwater populations of *Eurytemora carolleeae* (Atlantic clade of the *E. affinis* complex[38,69,70]). We first reared saline and freshwater populations under common garden conditions (5 PSU), to remove the effects of acclimation to native salinities. This intermediate salinity of 5 PSU represents a control that both populations can tolerate with ease. Then we transferred individuals from the saline and freshwater populations to one of the three treatment salinities (0, 5, or 15 PSU). The 0 PSU treatment (Lake Michigan water, 300 μS/cm) represented the native freshwater conditions, whereas the 15 PSU treatment represented a common salinity of the native saltmarsh habitat, where salinity fluctuates seasonally between 5 and 40 PSU. We then compared the saline and freshwater populations at the treatment salinities (0, 5, or 15 PSU) to determine evolutionary shifts between the populations in NKA immunolocalization and expression at these salinities (see STAR methods for details).

We examined the effects of the factors *Population* (saline versus freshwater populations), *Salinity* (0, 5, 15 PSU), and *Population* × *Salinity* interaction on the response variables *Body Size*, *Whole-Animal NKA*, *NKA IMG Area*, *NKA IMG Intensity*, and *Amount of NKA* (see specific results in the sections below). Our overall results revealed the presence of evolutionary shifts in NKA expression in the maxillary glands between ancestral saline and freshwater invading populations and acclimatory shifts in expression across salinities (Figures 2, 3, 4, 5, 6, and 7). We found evolutionary shifts in NKA expression both at the levels of the whole animal and *in situ* within the maxillary glands between ancestral saline and derived freshwater populations when reared under common garden salinities (0, 5, and 15 PSU). We also found acclimatory shifts in NKA expression in response to the different salinities in the saline population, but no significant plastic response in the freshwater population. As such, we observed the evolution of plasticity (i.e., evolution of reaction norms) from the ancestral saline to freshwater invading populations (significant *Population* × *Salinity* interaction), with the freshwater population exhibiting the evolution of canalization in NKA expression across salinities (see details in results sections below).

Body size varies across salinities

A shift in body size across salinities would suggest tradeoffs in energy allocation toward growth versus ionic regulation. We found a significant effect of the factor *Salinity* on *Body Size* (i.e., prosome length in μm) (Table S1A; two-way ANOVA; $F = 39.67$, df = 2, 283, $p < 0.0001$), with the smallest body size occurring at the lowest salinity (0 vs. 5 PSU: $p < 0.00319$, and 0 vs. 15 PSU: $p < 0.0001$) for both saline and freshwater

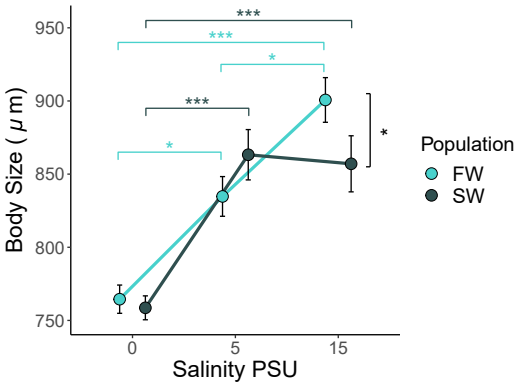

Figure 2. Variation in body size (i.e., prosome length) (μm) in response to treatment salinities (0, 5, and 15 PSU) for both saline and freshwater populations

Data are represented as mean ± SE (N = 289, FW: N = 41–48 per treatment salinity; SW: N = 42–57 per treatment salinity). Level of significance is indicated with asterisks (* = $p < 0.05$, *** = $p < 0.0001$). We found significant differences in *Body Size* in response to *Salinity* (two-way ANOVA; $F = 39.67$, df = 2, 283, $p < 0.0001$), with the smallest body size at the lowest salinity (0 PSU) (*post hoc* Tukey test; 0 vs. 5 PSU: $p < 0.00319$, and 0 vs. 15 PSU: $p < 0.0001$) for both saline and freshwater populations. *A priori* pairwise comparisons between saline and freshwater populations at each salinity revealed significant differences in *Body Size* between populations at 15 PSU (Student's t test; $t = 1.95$, df = 85, $p = 0.050$), with greater body size in the freshwater population. Notably, the effect of *Population* x *Salinity* on *Body Size* was significant (two-way ANOVA; $F = 3.02$, df = 2, 283, $p = 0.050$), indicating the evolution of plasticity in body size between the populations. Population means and standard errors are reported in Table S3.

populations (Figure 2). While the overall effect of *Population* on *Body Size* was not significant (Table S1A; two-way ANOVA; $F = 0.693$, df = 1, 284, $p = 0.406$), *a priori* population comparisons at each treatment salinity revealed that at the high salinity treatment (15 PSU) body size differed significantly between the freshwater and saline populations (Table S1A; Student's t test; $t = 1.95$, df = 85, $p = 0.050$), with a 1.05-fold larger body size in the freshwater population (mean difference = 43.6; strictly standardized mean difference = 0.263) (Figure 2). The interaction between *Population* and *Salinity* was significant (Table S1A; two-way ANOVA; $F = 3.02$, df = 2, 283, $p = 0.050$), indicating the evolution of plasticity in body size between the populations, with the freshwater population exhibiting greater plasticity in body size across salinities.

Whole-animal Na^+/K^+- ATPase protein expression is higher in the saline population under saline conditions

To identify the evolutionary and acclimatory shifts in the total amount of NKA protein extracted from whole animals, we performed a Western blot analysis comparing the saline and freshwater populations across three salinities (0, 5, 15 PSU). For quantifying the band intensities, we used as a control a "supermix," which was a mix of all treatment groups.[71,72] For each gel, we loaded an equal amount of this supermix and quantified the resulting supermix band to use as a reference. This supermix reference band served as a calibrator, allowing us to normalize variance in intensities within and among electrophoresis gels.

Our analysis used a total of 216 copepods, with 36 individuals per salinity treatment (0, 5, and 15 PSU), in groups of 6 individuals, for each population. *Salinity* had a significant effect on *Whole-Animal NKA* protein expression (Table S1B; two-way ANOVA: $F = 3.30$, df = 2, 34, $p = 0.0490$), as indicated by the immunoblot band signals (Figure 3A). *Whole-Animal NKA* protein signal intensity in the saline population was highest in the 15 PSU salinity treatment, relative to both the 0 and 5 PSU treatments (Figure 3B) (Table S1B; post hoc Tukey pairwise comparisons, 0 vs. 15 PSU, $p = 0.0169$ and 5 vs. 15 PSU, $p = 0.0444$). We found no significant effect of *Population* on *Whole-Animal NKA* (Table S1B; two-way ANOVA; $F = 0.805$, df = 1, 35, $p = 0.376$). However, *a priori* comparisons between the two populations at each treatment salinity did reveal that *Whole-Animal NKA* expression differed significantly between the populations at the 15 PSU treatment (Table S1B; Student's t test; $t = -2.17$, df = 11, $p = 0.050$), with higher NKA expression in the saline population relative to the freshwater population at 15 PSU (Figure 3B).

Na^+/K^+- ATPase is localized in the maxillary glands, based on whole mount immunostaining

Maxillary glands in crustaceans are typically located in the head region, specifically within the cephalosome (Figure 4). We localized NKA protein expression in the tubules and ducts of the maxillary glands in individual copepods, using *in toto* immunolocalization (Figures 5A–5C). This technique was used to visualize the distribution and localization of NKA within the entire animal. The intense staining of NKA in tubular structures at the base of the maxillae (feeding appendages) was consistent with the occurrence of maxillary glands at this location.[37,50] We also observed NKA in the copepod brain (Figure 5A, arrows), as well as subtle NKA staining in other non-osmoregulatory tissues, such as the muscles (Figures 5A and 5B). We saw no NKA staining in the coelomic sac or excretory duct of the maxillary glands. The staining of NKA in the maxillary gland cells appeared homogeneously fluorescent throughout the maxillary gland tubules and ducts. This homogeneous and even staining was consistent with the localization of NKA in the deep infoldings of the basolateral membrane of the ion transporting cells.[52] The localization of NKA in the basolateral membranes of the cells in the maxillary gland tubules and ducts supports the hypothesis that this organ is the site of reabsorption of ions from the primary urine to the hemolymph.

Evolution of plasticity of maxillary gland Na^+/K^+- ATPase expression from saline to freshwater populations

To determine evolutionary and acclimatory shifts in *in situ* expression of NKA in the maxillary glands, we performed *in situ* immunolocalization of NKA in both the saline and freshwater populations across salinity treatments (0, 5, and 15 PSU) (Figures 6 and 7). We made a total of 911 maxillary gland observations (i.e., quantified images of cuts) for 36 individuals, with six individuals at each treatment salinity, for both the saline and freshwater populations. We verified that every 5 μm cut that contained any portion of the maxillary glands was included in the analysis. We statistically analyzed the effects of the factors *Population* and *Salinity* on the response variable *Amount of NKA* within the tubular cells of the maxillary glands. This response variable is the product of "NKA immunolabeled maxillary gland area" (*NKA IMG Area*) and "NKA IMG

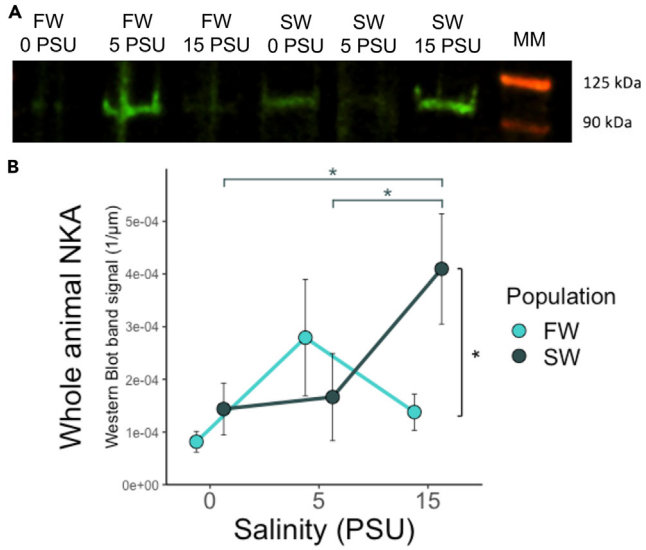

Figure 3. Whole-animal immunolabeled NKA protein expression in

E. carolleeae populations, showing evolutionary shifts between saline and freshwater populations and acclimatory shifts across treatment salinities (0, 5, and 15 PSU).

(A) Western blot membrane containing freshwater (FW) and saline (SW) populations at each treatment salinity (green bands) and a molecular marker (MM, red bands). (B) Whole-animal NKA protein expression, measured as integrated band signal intensity in saline and freshwater populations across the treatment salinities. Band signal intensity data were cube root transformed and normalized for the size of the animals (total prosome length in μm) and membrane variation (supermix band signal). Scale of the normalized band signal is measured as (pixel intensity of experimental band)/(pixel intensity of supermix band x total prosome length in μm). Data are represented as mean $\pm$ SE. Level of significance is indicated with asterisks (* = $p < 0.05$). *Salinity* had a significant effect on *Whole-Animal NKA* (two-way ANOVA: $F = 3.30$, df = 2,34, $p = 0.0490$). *A priori* comparisons of the two populations at each treatment salinity did reveal that *Whole-Animal NKA* was higher in saline copepods relative to freshwater copepods at the 15 PSU treatment salinity (Student's t test; $t = -2.17$, df = 11 $p = 0.050$). Population means and standard errors are reported in Table S3.

fluorescence intensity" (*NKA IMG Intensity*). We measured both the area and intensity of protein immunostaining, because these responses are not always correlated (e.g., large fluorescence area can have weak fluorescence intensity). However, in this study we found that *NKA IMG Area* and *NKA IMG Intensity* were significantly correlated (Pearson's correlation; $r = 0.636$, df = 35, $p < 0.0001$). Thus, we report the results for the response variable *Amount of NKA* (*NKA IMG Area* x *NKA IMG Intensity*), which accounts for both the area of the tubules in which NKA was expressed and how strongly NKA was expressed (Table 1).

For the response variable *Amount of NKA*, there was no significant effect of *Population* (Table 2; two-way ANOVA; $F = 2.54$, df = 1, 35, $p = 0.121$) or *Salinity* (Table 2; two-way ANOVA; $F = 1.39$, df = 2, 34, $p = 0.264$) (Figure 7). However, *a priori* comparisons between the populations at each treatment salinity did reveal significant differences in *Amount of NKA* at the 0 PSU rearing salinity (Student's t test, $t = -3.06$, df = 10, $p = 0.0119$) (Table 2), with the saline population showing 2.84-fold higher NKA expression than the freshwater population (mean difference = 2.61×10^5; strictly standardized mean difference = 1.21) (Table 1; Figures 6 and 7). This population level difference in NKA expression at 0 PSU can be attributed to both the *NKA IMG Area* and *NKA IMG Intensity*, as the populations showed significant differences for both response variables (*NKA IMG Area*; Table S2-A; Student's t test; $t = -2.83$, df = 10, $p = 0.0181$; *NKA IMG Intensity*; Table S2-B; Wilcoxon rank-sum test; $W = 5$, $n_1 = 6$, $n_2 = 6$, $p = 0.0411$), with the saline population showing higher values at 0 PSU (Figures S1A and S1B).

Notably, we found the evolution of plasticity in response to salinity between the saline and freshwater populations. The *Population* × *Salinity* interaction had a significant effect on the *Amount of NKA* in the maxillary glands (Table 2; two-way ANOVA; $F = 3.69$, df = 2, 34, $p = 0.0364$), indicating that the populations differed significantly in their plastic responses to changes in salinity (Figures 6 and 7). This result was attributed largely to the significant effect of *Population* x *Salinity* on *NKA IMG Area* (Table S2-A; two-way ANOVA; $F = 3.17$, df = 2, 34, $p = 0.050$) (Figure S1-A). *NKA IMG Intensity* showed the same trend but was not significant on its own (Table S2-B; Kruskal-Wallis rank-sum test; $H = 7.70$, df = 5, $p = 0.174$).

The ancestral saline population showed greater plasticity in response to salinity change, with canalization (lower plasticity) in the derived freshwater population (Figure 7). Pairwise *a priori* comparisons between the salinity treatments revealed no significant differences in *Amount of NKA* for each population (Table 2; Student's t test; $p > 0.05$ for all salinities) (Figure 7). However, for *NKA IMG Area*, which is a component of *Amount of NKA* (see above), pairwise *a priori* comparisons between salinity treatments did reveal a significant difference between the 0 PSU and 15 PSU treatments for the saline population (Table S2-A; Student's t test; $t = 2.47$, df = 11, $p = 0.0332$), with higher *NKA IMG Area* at 0 PSU (Figure S1-A). In contrast, there was no significant difference in *NKA IMG Area* between salinities for the freshwater population (Table S2-A: Student's t test; $p > 0.05$ for all salinities). These results indicate greater plasticity in *NKA IMG Area* in the saline population than in the freshwater population (Figure S1).

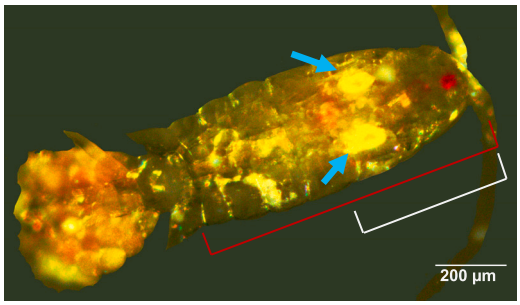

Figure 4. Brightfield image of the dorsal view of an adult female *E carolleeae* copepod from the freshwater population reared at 5 PSU

Prosome length is indicated by the red bracket and cephalosome length is indicated by the white bracket. The maxillary glands are indicated by the blue arrows.

In addition, *Amount of NKA* expression within the maxillary gland tubule cells showed higher variance among the salinity treatments in the saline population (coefficient of variation = 43.5%) than in the freshwater population (coefficient of variation = 17.0%) (Figure 6). In particular, *Amount of NKA* expressed at the 0 PSU treatment was ~2-fold greater than at the higher salinities (0 vs. 5 PSU = 1.9-fold; 0 vs. 15 PSU = 2.25-fold) (Table 1; Figures 6 and 7). In contrast, the freshwater population exhibited more similar levels of NKA expression in the tubules across salinities (0 vs. 5 PSU = 1.1-fold; 0 vs. 15 PSU = 1.4-fold) (Table 1; Figures 6 and 7). Thus, together, these results indicate the evolution of plasticity in salinity response from saline to freshwater populations, with greater plasticity in the saline population and the evolution of canalization in the freshwater population.

DISCUSSION

The rise of biological invasions is of enormous ecological and environmental concern, contributing to the current mass extinction event.[16,17,19,20,73] Notably, a large proportion of highly prolific freshwater invading populations have originated from saline habitats,[14–16] likely through the transport and discharge of ship ballast water in inland ports.[18,21,22,74,75] In addition, habitat salinity is rapidly changing across the globe due to climate change.[4,6,8,9,11,76] In such cases, adaptation to rapid salinity change becomes paramount, as the failure to do so would lead to likely extinction in the novel habitat for many species.

Here, we investigated the evolution of ion regulatory mechanisms involved in freshwater adaptation following a saline to freshwater invasion event. The novel feature of this study is in examining the evolution of *in situ* ion transporter protein expression patterns following habitat change. We examined protein localization at the organ and cellular levels, particularly in the poorly understood copepod maxillary glands. We compared *in situ* NKA expression between two populations of *Eurytemora carolleeae*, specifically an ancestral saline population from its native range in the St. Lawrence estuary salt marsh, where salinity can fluctuate seasonally between 5 and 40 PSU, and a derived invasive freshwater population in Lake Michigan, residing in relatively stable freshwater conditions close to 0 PSU (conductivity of 300 μS/cm). Here, we revealed both the evolution of NKA expression between the saline and freshwater populations, as well as acclimatory shifts in NKA expression across salinities (Figures 3, 6, and 7; Tables 1; 2, S1, S2, and S3). Moreover, we discovered the evolution of plasticity between the two populations, with the ancestral saline population exhibiting a relatively large plastic response across salinities and the freshwater invading population displaying the evolution of reduced plasticity (Figures 6 and 7; Tables 2 and S2A-B). As such, this study reveals the evolutionary shifts likely associated with the evolution of physiological function during salinity change, involving the evolution of ion transporter NKA expression in an organ putatively involved in ion reabsorption.

Plasticity in body size across salinities

Ionic regulation in freshwater environments is energetically costly, given the consumption of ATP required to perform active ion uptake from a dilute environment, deficient of ions such as Na^+ and Cl^-.[77] In populations of the *E. affinis* species complex, both saline and freshwater populations hyperosmoregulate (maintain higher hemolymph osmolality than the environment) when reared in fresh water, with freshwater populations maintaining higher hemolymph osmolality than their ancestral saline populations.[26] Thus, the energetic costs of maintaining this high hemolymph osmolality in the freshwater populations under low-salinity conditions would be expected to be exceedingly high.

Our results of smaller body size at 0 PSU relative to higher salinities (5 and 15 PSU) for both saline and freshwater populations (Figure 2) might be linked to the high energetic cost of ion uptake at lower salinities. This result might be attributed to tradeoffs between energy allocation for growth versus hyperosmoregulation under freshwater conditions.[78] The reduction in resource allocation toward growth is likely correlated with lower fecundity, given the positive correlation found between body size and fecundity in the Europe clade of the *E. affinis* species complex.[79] Reaction norm experiments in brackishwater copepods have also revealed lower fecundity when copepods were reared at low (0–2.5 PSU) relative to higher salinities (10–20 PSU).[80]

We observed the evolution of plasticity in body size between the populations (Figure 2), indicated by the significant *Population* × *Salinity* interaction (Table S1-A), with greater plasticity in the freshwater population. The greater plasticity in the freshwater population was attributable to the larger body size in the freshwater copepods at 15 PSU, relative to the other salinities and relative to the saline population. This greater plasticity in body size in the freshwater population was in contrast to the reduced plasticity in NKA *in situ* expression (Figure 7).

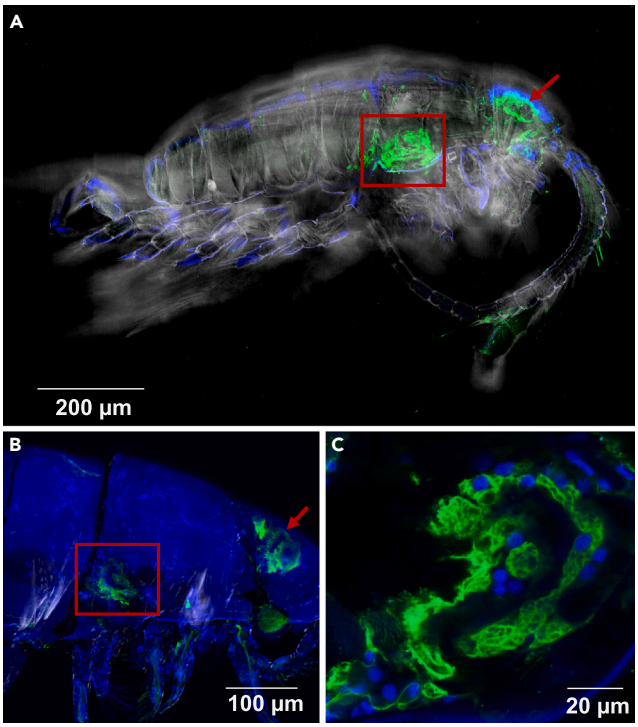

Figure 5. *In toto* Na^+/K^+- ATPase (NKA) immunostaining in adult *E carolleeae* copepods with bright field, DAPI (blue), and NKA (green) filters

(A) A male copepod from the saline population reared at 0 PSU showing the NKA immunostained area of the maxillary gland (red square). The brain is also brightly stained with NKA (red arrow).

(B) Maxillary gland of an adult male copepod from the saline population reared at 15 PSU.

(C) NKA immunostained area, corresponding to the tubules and ducts of the maxillary gland of a female copepod from the freshwater population reared at 0 PSU.

Evolution of Na^+/K^+- ATPase expression in the maxillary glands between saline and freshwater populations

The maxillary glands are thought to play a role in urine production and regulating the ionic concentration and volume of the urine released.[37,50] These functions resemble those of antennal glands in decapod crustaceans and vertebrate kidneys.[37,66] The structure and composition of maxillary glands are often linked to substantial ion transport activity and the production of dilute urine in freshwater organisms,[25,33,37,67] indicating a potential involvement in ionic and hydric regulation.

Given the putative role of the maxillary glands in osmoregulation, we hypothesized that the maxillary glands would play a key role in freshwater adaptation. Thus, we had predicted that NKA expression would be higher in the freshwater population under freshwater conditions, relative to its saline ancestor, as a mechanism of freshwater adaptation. Surprisingly, we found significantly higher *in situ* NKA expression in the maxillary glands of the saline population at the low salinity (0 PSU) treatment, relative to the freshwater population (Figure 7). This result opposed our hypothesis that maxillary glands serve a key role in freshwater adaptation. We also hypothesized that NKA expression in the maxillary glands would be higher at low salinities, relative to higher salinities, as an acclimatory response to ion poor conditions. However, while we found an acclimatory response (plasticity) across salinities in the saline population, we found a canalized response (no plasticity) in the freshwater population.

This surprising finding, of reduced NKA expression in the maxillary glands of freshwater population at 0 PSU, relative to the saline population, suggests that freshwater populations *of E. carolleae* might have evolved alternative mechanisms to maintain elevated internal ionic concentrations in their low salinity environment. One evolved mechanism might be increased ion uptake from the environment. This increased ion uptake activity might involve NKA and other ion transporters in the Crusalis organs of the swimming legs.[25,51,52] An additional contributing mechanism might be to mitigate ionic losses in the freshwater populations, such as by reducing integument permeability, thereby minimizing passive water influx and diffusive ion efflux. In decapods, permeability coefficients are 100 times lower for Na^+ and 50–500 lower for water in the cuticle lining of the gills, hindgut, and carapace in osmoregulating freshwater species, relative to most saline species that are categorized as osmoconformers.[30] In *E. carolleeae*, ion efflux assays using radioactive Na^+ suggest that the integument of the freshwater population is less permeable to ionic losses, relative to the saline ancestor (Figure S2 and Table S4). The evolution of paracellular permeability (i.e., conductance of water and small solutes through spaces between adjacent epithelial cells) in *E. affinis* complex populations warrants further exploration, potentially elucidating its role alongside other mechanisms that promote ion retention in freshwater populations.

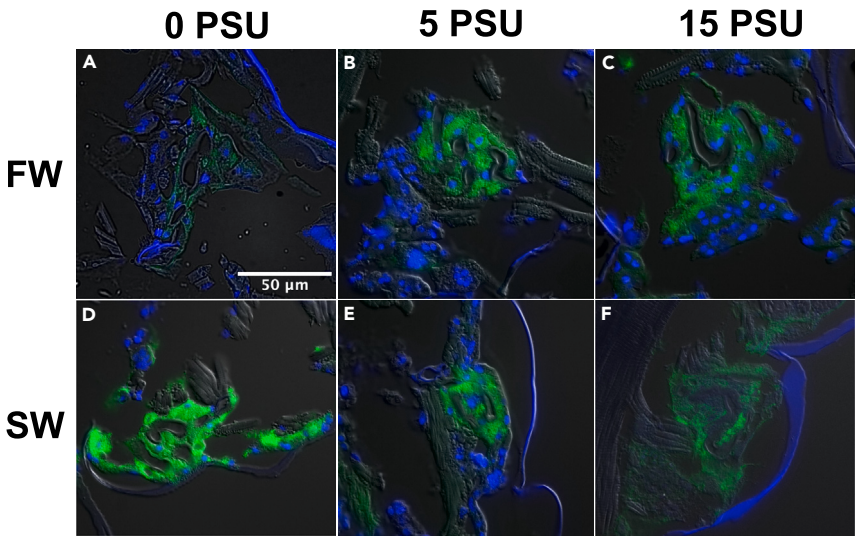

Figure 6. Maxillary gland fluorescence intensity of NKA (green) for saline (SW) and freshwater (FW) populations under common garden treatment salinities (0, 5, and 15 PSU)

These images also depict the cell nuclei with DAPI (blue) and brightfield background. Exposure time and magnification were kept uniform for all images. Panels A–F are all adult females from each population reared at the corresponding salinities.

Most notably, we found the evolution of plasticity in NKA maxillary gland expression between the saline and freshwater populations, as reflected by the significant *Population* × *Salinity* interaction (Figure 7 and S1-A; Table 2). The evolution of the canalization of NKA expression across salinities in the freshwater population was especially striking. The higher NKA expression in the saline population at 0 PSU relative to 15 PSU (Figure S1-A and Table 2) indicated a significant acclimatory response to salinity change. In contrast, the lack of significant differences in NKA expression between salinities in the freshwater population (Tables 2 and S2A-B) indicated the loss of this plasticity and the evolution of canalization.

The higher plasticity observed in NKA expression of the saline population, relative to the freshwater population, might arise from its evolutionary history in a habitat with seasonal and daily variation in salinity in their tidal marsh environment.[53,55] Phenotypic plasticity, where organisms express a range of phenotypes across different environments, may provide fitness advantages that allow the populations to persist under fluctuating conditions.[68,81,82] In response to radical environmental change, such as the introduction into a novel freshwater habitat, the genotype with extreme plasticity, including greater freshwater tolerance, would be favored by selection.[82,83] Several models predict the genetic assimilation of plasticity following invasion into the novel habitat, where selection for the optimum phenotype would lead to canalization over time scales of 10,000–100,000 generations.[82–84] Such selection for reduced plasticity could occur if the new environment is stable and there is a "cost" to maintaining plasticity,[85] or if there is relaxed selection and plasticity is lost due to genetic drift. In the case of *E. affinis* complex populations, previous reaction norm studies suggest that there is a cost to plasticity, given the presence of tradeoffs between saline and freshwater tolerance.[56,86,87] Given that the freshwater population was introduced into the Great Lakes only ~65 years ago, the reduction in plasticity we found in NKA expression in the maxillary glands has transpired over a relatively short time span of fewer than 500 generations. This observation suggests that the cost of NKA expression in the maxillary glands is high, possibly favoring selection for its reduced expression following colonization into a relatively constant freshwater habitat.

This loss of plasticity in NKA expression in the freshwater population contrasts sharply with the evolution of increased plasticity previously observed in whole-body V-type H^+ ATPase (VHA) activity in freshwater *E. affinis* complex populations.[56] This prior study found higher plasticity in VHA activity in freshwater populations (of both the Atlantic and Gulf clades) than in the saline populations, with the highest activity under freshwater conditions.[56] NKA and VHA are both ATPases that are energetically highly costly,[88] such that the evolution of increased plasticity of VHA activity in freshwater populations but the loss of plasticity in NKA expression in the maxillary gland is intriguing. VHA is a primary active transporter that drives sodium uptake from the environment in osmoregulatory epithelia, such as the gills,[89] and is hypothesized to drive sodium uptake in *E. affinis* complex populations.[25,51,52] The evolution of increased plasticity of VHA activity in the freshwater population might arise from selection favoring the extreme plastic trait for VHA-facilitated sodium uptake, with higher VHA activity under freshwater conditions, during freshwater invasions.[56,82,83] Selection on NKA plasticity in the maxillary glands, where ion reabsorption likely takes place, might be far less critical during freshwater adaptation. Thus, adaptation to different salinity habitats might involve energetic allocation toward different ion transporters and their plasticity in different environments.

Whole-animal versus *maxillary gland* Na^+/K^+- ATPase *expression*

The ion transporter enzyme NKA is involved in multiple physiological functions, including osmoregulation, generation of the cell action potential, maintenance of muscle function, and intestinal nutrient absorption.[90,91] Given the diverse roles of NKA, whole-animal assays of NKA

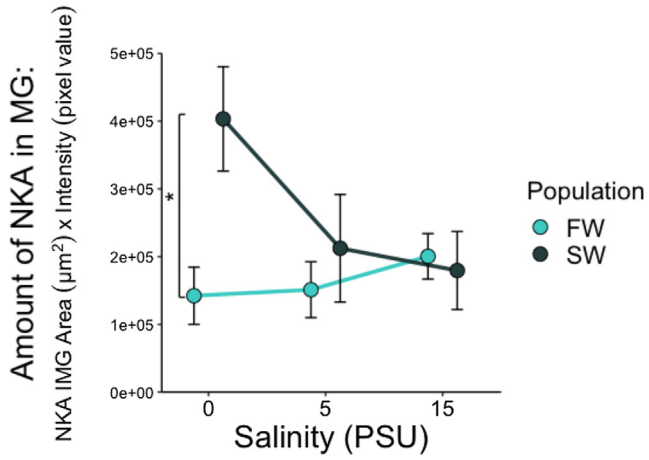

Figure 7. Shifts in NKA *in situ* expression in the maxillary glands (MG) in response to treatment salinities (0, 5, 15 PSU) for both the freshwater (FW) and saline (SW) populations

The response variable *Amount of NKA* is the product of *NKA IMG Area* and *NKA IMG Intensity*. *NKA IMG Area* refers to the volume (μ^3) of the maxillary glands (MG) expressing NKA, standardized by the prosome length (μm), whereas *NKA IMG Intensity* indicates the florescence strength of NKA expression in the MG. Data are represented as Mean $\pm$ propagated SE. Level of significance is indicated with asterisks (* = $p < 0.05$). While the overall effect of *Population* on *Amount of NKA* expression was not significant (two-way ANOVA; $F = 2.54$, df = 1, 35, $p = 0.121$), *a priori* comparisons between the populations at each salinity revealed significant differences at the 0 PSU treatment (Student's t test, $t = -3.06$, df = 10, $p = 0.0119$). The effect of *Salinity* on *Amount of NKA* expression was not significant (two-way ANOVA; $F = 1.39$, df = 2,34, $p = 0.264$). Notably, the effect of *Population* x *Salinity* on *Amount of NKA* expression was significant (two-way ANOVA; $F = 3.69$, df = 2, 34, $p = 0.0364$), indicating the evolution of plasticity between the saline and freshwater populations. Population means and standard errors are reported in Table 1.

would capture all of these functions. Therefore, we would not expect "whole-animal" NKA expression to reflect the expression of NKA specifically involved in osmoregulation. However, it was still somewhat surprising that both the saline and freshwater populations showed lowest "whole-animal" NKA expression at 0 PSU (Figure 3), a salinity expected to involve considerable hyperosmoregulation and need for ion retention and reabsorption.

Notably, whole-body NKA expression was significantly higher in the saline population than in the freshwater population at 15 PSU, but not at 0 and 5 PSU (Figure 3). This finding was partially consistent with a previous study, where whole-body NKA enzyme activity was significantly higher across all rearing salinities (0, 5, and 15 PSU) in the saline populations relative to the derived freshwater populations of the Atlantic and Gulf clades of *E. affinis* complex.[56] The observed lack of correlation between whole-body NKA expression and NKA enzyme activity at 0 and 5 PSU might be due to lower statistical power in this study. Alternatively, lack of correlation between NKA enzyme expression and activity could arise from post translational processes at certain salinities (i.e., phosphorylation)[92] that could alter NKA activity without changing its protein expression.

Interestingly, patterns of NKA expression differed sharply between the maxillary glands (Figure 7) and the whole animal (Figure 3). For the saline population NKA expression in the maxillary glands was highest at 0 PSU, in contrast to the highest whole-body NKA expression at 15 PSU. Therefore, our findings emphasize the importance of conducting *in situ* analyses of NKA in specific tissues and organs. While the whole-body assays capture expression induced by all the functions of all the paralogs of NKA, *in situ* measurements of NKA expression in specific organs, such as the maxillary glands, would reflect specific functions of NKA. Presumably, the evolutionary and acclimatory patterns of *in situ* NKA expression we found in the maxillary glands reflect the putative role that NKA plays in ion reabsorption, as an important component of osmoregulation and salinity adaptation. Demonstrating that the heritable differences observed between the saline and freshwater populations are the result of evolutionary adaptation would require further investigation. Additional experiments would be essential to conclusively establish the link between the observed heritable shifts in NKA expression and their impacts on fitness or physiological function. We have found that NKA alleles are targets of selection in wild populations and laboratory selection lines in response to changes in salinity.[49,53] Our future studies will examine the association between NKA alleles and paralogs with NKA ion transport function and related impacts on survival at different salinities.

Limitations of this study

This study, while providing valuable insights into NKA expression across salinities, does not distinguish among patterns of expression for different NKA paralogs. There are ~6 NKA-alpha paralogs (and likely one pseudogene) present in *E. affinis* complex genomes.[93] Our study used an immunoreactive antibody that binds to a highly conserved region in the NKA-α protein. Thus, this antibody is likely binding to a region conserved among several, if not all, of the NKA-α paralogs. Functions among NKA paralogs likely vary, reflected in the divergent patterns of gene expression evolution between saline and freshwater populations among the different paralogs.[55] For instance, our prior study found

Table 1. Mean values of Na^+/K^+-ATPase (NKA) expression of freshwater and saline populations across three salinities (0, 5, 15 PSU)

Population	Salinity (PSU)	Mean ± SD ($x10^5$)
Saline	0	4.03 ± 0.77
Freshwater	0	1.42 ± 0.42
Saline	5	2.12 ± 0.79
Freshwater	5	1.51 ± 0.41
Saline	15	1.79 ± 0.58
Freshwater	15	2.00 ± 0.34

Amount of NKA expression in the maxillary glands is quantified as the product of *NKA IMG Area* x *NKA IMG Intensity*. Mean values and standard deviation of the mean (SD) are reported. The standard deviation values reflect the propagated error for the product between *NKA IMG Area* and *Intensity* calculated as: $SD = \sigma_x/\mu_x = \sqrt{((\sigma_a/\mu_a)^2 + (\sigma_b/\mu_b)^2)}$, Where σ = standard deviation, μ = mean, subscripts x = *Amount of NKA*, a = *NKA IMG Area*, and b = *NKA IMG Intensity*.

that the paralog *NKA-α−1* is more highly expressed in the freshwater population relative to the saline population at 0 PSU and 15 PSU. Conversely, *NKA-α−2* is more highly expressed in the saline population at 0 PSU.[55] Our use of a highly conserved NKA antibody reveals how the NKA paralogs collectively respond to salinity, but obscures the contributions of each individual paralog. Thus, future studies would need to use antibody probes specific to each NKA paralog to determine functional differentiation and functional evolution for each paralog.

STAR★METHODS

Detailed methods are provided in the online version of this paper and include the following:

- KEY RESOURCES TABLE
- RESOURCE AVAILABILITY
  - Lead contact
  - Materials availability
  - Data and code availability
- EXPERIMENTAL MODEL AND STUDY PARTICIPANT DETAILS
  - Population sampling
- METHOD DETAILS
  - Common garden experimental design

Table 2. Statistical results for comparisons of *in situ* Na^+/K^+-ATPase (NKA) expression in the maxillary glands between freshwater and saline populations across three salinities (0, 5, 15 PSU)

Comparison (greater value indicated by >)	Test statistic	df	*p*-value
Population	$F = 2.54$	1, 35	0.121
0 PSU, saline > fresh population	$t = -3.06$	10	0.0119*
5 PSU	$t = -0.169$	10	0.869
15 PSU	$t = 0.249$	11	0.808
Salinity	$F = 1.39$	2, 34	0.264
Saline population, 0 vs. 5 PSU	$t = 2.17$	10	0.0553
Saline population, 0 vs. 15 PSU	$t = 1.89$	10	0.0884
Saline population, 5 vs. 15 PSU	$t = -0.579$	10	0.577
Freshwater population, 0 vs. 5 PSU	$t = -0.546$	10	0.598
Freshwater population, 0 vs. 15	$t = -1.66$	11	0.133
Freshwater population, 5 vs. 15 PSU	$t = -1.28$	11	0.228
Population × *Salinity* interaction	$F = 3.69$	2, 34	0.0364*

Amount of NKA expression in the maxillary glands was quantified as the product of *NKA IMG Area* x *NKA IMG Intensity*. Statistical significance of comparisons were determined using a two-way ANOVA and *a priori* pairwise Student's t-tests. Data were square root transformed to satisfy normality requirements. Results show effects of the factors *Population* (saline vs. freshwater populations), *Salinity* (0, 5, 15 PSU), and the interaction of *Population* × *Salinity* on Na^+/K^+-ATPase expression. F = test statistic from the ANOVA and t = test statistic from Student's t-tests, and df = degrees of freedom. Significant differences were observed at $p < 0.05$ = *.

SUPPLEMENTAL INFORMATION

Supplemental information can be found online at https://doi.org/10.1016/j.isci.2024.110278.

ACKNOWLEDGMENTS

This project was funded by the French National Research Agency ANR-19-MPGA-0004 (Macron's "Make Our Planet Great Again" award), National Science Foundation grants OCE-1658517, and NSF DEB-2055356 to Carol E. Lee. Elodie Jublanc and Vicky Diakou from the Montpellier Resource Imagerie (MRI) provided guidance, maintenance, and support when using the microscopes. Greg Gelembiuk shared his data and observations on integument permeability of *E. carolleeae* populations. Grégoire Cortial and Gesche Winkler performed sample collections of the saline population from Baie de L'Isle Verte in the St. Lawrence estuary, Quebec, Canada. Antoine Fraimout, Benny Kleinerman, Delphine Bonnet, and Romain Gros helped with water collection and lab maintenance during animal culturing.

AUTHOR CONTRIBUTIONS

Methodology and experimental design: TEP, CEL, and CLN; processing of data and statistical approach and analysis: TEP and CEL; animal care and experimentation: TEP, JFR, EM, and CB; experimentation and data acquisition: TEP, SH, and WZ; writing of original draft: TEP, CEL, and CLN; writing, reviewing, and editing: TEP, CEL, GC, and CLN; supervision: CEL and CLN; funding acquisition: CEL. All authors reviewed and approved the article.

DECLARATION OF INTERESTS

The authors have no competing interests.

Received: March 4, 2024
Revised: April 24, 2024
Accepted: June 13, 2024
Published: June 17, 2024

REFERENCES

1. Kubelka, V., Sandercock, B.K., Székely, T., and Freckleton, R.P. (2022). Animal migration to northern latitudes: Environmental changes and increasing threats. Trends Ecol. Evol. *37*, 30–41. https://doi.org/10.1016/j.tree.2021.08.010.
2. Popp, T., and Wilber, D.H. (2021). Associations between winter temperatures and the timing and duration of annual larval recruitment of a non-native anomuran crab. Estuar. Coast *44*, 1074–1082. https://doi.org/10.1007/s12237-020-00831-z.
3. Simberloff, D., and Rejmánek, M. (2011). In Encyclopedia of Biological Invasions, D. Simberloff and M. Rejmánek, eds. (University of California Press).
4. Durack, P.J., Wijffels, S.E., and Matear, R.J. (2012). Ocean salinities reveal strong global water cycle intensification during 1950 to 2000. Science *336*, 455–458. https://doi.org/10.1126/science.1212222.
5. Siepielski, A.M., Morrissey, M.B., Buoro, M., Carlson, S.M., Caruso, C.M., Clegg, S.M., Coulson, T., Dibattista, J., Gotanda, K.M., Francis, C.D., et al. (2017). Precipitation drives global variation in natural selection. Science *355*, 959–962. https://doi.org/10.1126/science.aag277.
6. Durack, P. (2015). Ocean salinity and the global water cycle. Oceanography *28*, 20–31. https://doi.org/10.5670/oceanog.2015.03.
7. Durack, P.J., Gleckler, P.J., Landerer, F.W., and Taylor, K.E. (2014). Quantifying underestimates of long-term upper-ocean warming. Nat. Clim. Chang. *4*, 999–1005. https://doi.org/10.1038/nclimate2389.
8. Meier, H.E.M., Kjellström, E., and Graham, L.P. (2006). Estimating uncertainties of projected Baltic Sea salinity in the late 21st century. Geophys. Res. Lett. *33*, 1–4. https://doi.org/10.1029/2006GL026488.
9. Kniebusch, M., Meier, H.M., and Radtke, H. (2019). Changing salinity gradients in the Baltic Sea as a consequence of altered freshwater budgets. Geophys. Res. Lett. *46*, 9739–9747. https://doi.org/10.1029/2019GL083902.
10. Kankaanpää, H.T., Alenius, P., Kotilainen, P., and Roiha, P. (2023). Decreased surface and bottom salinity and elevated bottom temperature in the Northern Baltic Sea over the past six decades. Sci. Total Environ. *859*, 160241. https://doi.org/10.1016/j.scitotenv.2022.160241.
11. Schroeder, K., Chiggiato, J., Bryden, H.L., Borghini, M., and Ben Ismail, S. (2016). Abrupt climate shift in the Western Mediterranean Sea. Sci. Rep. *6*, 23009. https://doi.org/10.1038/srep23009.
12. Schroeder, K., Chiggiato, J., Josey, S.A., Borghini, M., Aracri, S., and Sparnocchia, S. (2017). Rapid response to climate change in a marginal sea. Sci. Rep. *7*, 4065. https://doi.org/10.1038/s41598-017-04455-5.
13. Lee, C.E., Downey, K., Colby, R.S., Freire, C.A., Nichols, S., Burgess, M.N., and Judy, K.J. (2022). Recognizing salinity threats in the climate crisis. Integr. Comp. Biol. *62*, 441–460. https://doi.org/10.1093/icb/icac069.
14. Lee, C.E., and Bell, M.A. (1999). Causes and consequences of recent freshwater invasions by saltwater animals. Trends Ecol. Evol. *14*, 284–288. https://doi.org/10.1016/S0169-5347(99)01596-7.
15. Casties, I., Seebens, H., and Briski, E. (2016). Importance of geographic origin for invasion success: A case study of the North and Baltic Seas versus the Great Lakes–St. Lawrence River region. Ecol. Evol. *6*, 8318–8329. https://doi.org/10.1002/ece3.2528.
16. Ricciardi, A. (2006). Patterns of invasion in the Laurentian Great Lakes in relation to changes in vector activity. Divers. Distrib. *12*, 425–433. https://doi.org/10.1111/j.1366-9516.2006.00262.x.

17. Spidle, A.P., Marsden, J.E., and May, B. (1994). Identification of the Great Lakes quagga mussel as *Dreissena bugensis* from the Dnieper River, Ukraine, on the basis of allozyme variation. Can. J. Fish. Aquat. Sci. *51*, 1485–1489. https://doi.org/10.1139/f94-148.
18. Cristescu, M.E.A., Hebert, P.D.N., Witt, J.D.S., MacIsaac, H.J., and Grigorovich, I.A. (2001). An invasion history for *Cercopagis pengoi* based on mitochondrial gene sequences. Limnol. Oceanogr. *46*, 224–229. https://doi.org/10.4319/lo.2001.46.2.0224.
19. Ruiz, G.M., Carlton, J.T., Grosholz, E.D., and Hines, A.H. (1997). Global invasions of marine and estuarine habitats by non-indigenous species: Mechanisms, extent, and consequences. Am. Zool. *37*, 621–632. https://doi.org/10.1093/icb/37.6.621.
20. Moyle, P.B., and Light, T. (1996). Biological invasions of fresh water: Empirical rules and assembly theory. Biol. Conserv. *78*, 149–161. https://doi.org/10.1016/0006-3207(96)00024-9.
21. May, G.E., Gelembiuk, G.W., Panov, V.E., Orlova, M.I., and Lee, C.E. (2006). Molecular ecology of zebra mussel invasions. Mol. Ecol. *15*, 1021–1031. https://doi.org/10.1111/j.1365-294X.2006.02814.x.
22. Gelembiuk, G.W., May, G.E., and Lee, C.E. (2006). Phylogeography and systematics of zebra mussels and related species. Mol. Ecol. *15*, 1033–1050. https://doi.org/10.1111/j.1365-294X.2006.02816.x.
23. Lee, C.E., Remfert, J.L., Opgenorth, T., Lee, K.M., Stanford, E., Connolly, J.W., Kim, J., and Tomke, S. (2017). Evolutionary responses to crude oil from the Deepwater Horizon oil spill by the copepod *Eurytemora affinis*. Evol. Appl. *10*, 813–828. https://doi.org/10.1111/eva.12502.
24. Remane, A. (1971). In Biology of Brackish Water, Second Edition, A. Remane, C. Schlieper, and C. Schlieper, eds. (John Wiley and Sons).
25. Lee, C.E., Charmantier, G., and Lorin-Nebel, C. (2022). Mechanisms of Na^+ uptake from freshwater habitats in animals. Front. Physiol. *13*, 1006113. https://doi.org/10.3389/fphys.2022.1006113.
26. Lee, C.E., Posavi, M., and Charmantier, G. (2012). Rapid evolution of body fluid regulation following independent invasions into freshwater habitats. J. Evol. Biol. *25*, 625–633. https://doi.org/10.1111/j.1420-9101.2012.02459.x.
27. Charmantier, G., Charmantier-Daures, M., and Towle, D. (2009). Osmotic and ionic regulation in aquatic arthropods. In Osmotic and Ionic Regulation. Cells and Animals, Evans (CRC Press), pp. 165–320. https://doi.org/10.1201/9780849380525.
28. Lee, C.E. (2002). Evolutionary genetics of invasive species. Trends Ecol. Evol. *17*, 386–391. https://doi.org/10.1016/S0169-5347(02)02554-5.
29. Lee, C.E. (2011). Evolution of invasive populations. In Encyclopedia of Biological Invasions, D. Simberloff and M. Rejmánek, eds. (University of California Press), pp. 215–222.
30. Péqueux, A. (1995). Osmotic Regulation in Crustaceans. J. Crustac Biol. *15*, 1–60.
31. Dymowska, A.K., Hwang, P.P., and Goss, G.G. (2012). Structure and function of ionocytes in the freshwater fish gill. Respir. Physiol. Neurobiol. *184*, 282–292. https://doi.org/10.1016/j.resp.2012.08.025.
32. Zimmer, A.M., and Perry, S.F. (2022). Physiology and aquaculture: A review of ion and acid-base regulation by the gills of fishes. Fish Fish. *23*, 874–898. https://doi.org/10.1111/faf.12659.
33. Khodabandeh, S., Charmantier, G., and Charmantier-Daures, M. (2005). Ultrastructural studies and Na^+, K^+-ATPase immunolocalization in the antennal urinary glands of the lobster *Homarus gammarus* (Crustacea, Decapoda). J. Histochem. Cytochem. *53*, 1203–1214. https://doi.org/10.1369/jhc.4A6540.2005.
34. Tsai, J.R., and Lin, H.C. (2014). Functional anatomy and ion regulatory mechanisms of the antennal gland in a semi-terrestrial crab, *Ocypode stimpsoni*. Biol. Open *3*, 409–417. https://doi.org/10.1242/bio.20147336.
35. Anger, K. (1995). The conquest of freshwater and land by marine crabs: adaptations in life-history patterns and larval bioenergetics. J. Exp. Mar. Biol. Ecol. *193*, 119–145.
36. Anger, K. (2016). Adaptation to Life in Fresh Water by Decapod Crustaceans: Evolutionary Challenges in the Early Life-History Stages. In A Global Overview of the Conservation of Freshwater Decapod Crustaceans, T. Kawai and N. Cumberlidge, eds. (Springer International Publishing), pp. 127–168. https://doi.org/10.1007/978-3-319-42527-6_5.
37. Freire, C.A., Onken, H., and McNamara, J.C. (2008). A structure-function analysis of ion transport in crustacean gills and excretory organs. Comp. Biochem. Physiol. Mol. Integr. Physiol. *151*, 272–304. https://doi.org/10.1016/j.cbpa.2007.05.008.
38. Lee, C.E. (1999). Rapid and repeated invasions of fresh water by the copepod *Eurytemora affinis*. Evolution *53*, 1423–1434. https://doi.org/10.2307/2640889.
39. Winkler, G., Dodson, J.J., and Lee, C.E. (2008). Heterogeneity within the native range: Population genetic analyses of sympatric invasive and noninvasive clades of the freshwater invading copepod *Eurytemora affinis*. Mol. Ecol. *17*, 415–430. https://doi.org/10.1111/j.1365-294X.2007.03480.x.
40. Heinle, D.R., and Flemer, D.A. (1975). Carbon requirements of a population of the estuarine copepod *Eurytemora affinis*. Mar. Biol. *31*, 235–247.
41. Oesmann, S., and Thiel, R. (2001). Feeding of juvenile twaite shad (*Alosa fallax* Lacépède, 1803) in the Elbe estuary. Bull. Fr. Pêche Piscic. *362/363*, 785–800. https://doi.org/10.1051/kmae:2001019.
42. Paulsen, M., Clemmesen, C., Hammer, C., Polte, P., and Malzahn, A.M. (2017). Food-limited growth of larval Atlantic herring *Clupea harengus* recurrently observed in a coastal nursery area. Helgol. Mar. Res. *70*, 17. https://doi.org/10.1186/s10152-016-0470-y.
43. Lee, C.E. (2016). Evolutionary mechanisms of habitat invasions, using the copepod *Eurytemora affinis* as a model system. Evol. Appl. *9*, 248–270. https://doi.org/10.1111/eva.12334.
44. Almén, A.K., Vehmaa, A., Brutemark, A., Bach, L., Lischka, S., Stuhr, A., Furuhagen, S., Paul, A., Bermúdez, J.R., Riebesell, U., and Engström-Öst, J. (2016). Negligible effects of ocean acidification on *Eurytemora affinis* (Copepoda) offspring production. Biogeosciences *13*, 1037–1048. https://doi.org/10.5194/bg-13-1037-2016.
45. Souissi, A., Souissi, S., and Hwang, J.S. (2016). Evaluation of the copepod *Eurytemora affinis* life history response to temperature and salinity increases. Zool. Stud. *55*, e4. https://doi.org/10.6620/ZS.2016.55-04.
46. Karlsson, K., and Winder, M. (2020). Adaptation potential of the copepod *Eurytemora affinis* to a future warmer Baltic Sea. Ecol. Evol. *10*, 5135–5151. https://doi.org/10.1002/ece3.6267.
47. Ketzner, P.A., and Bradley, B.P. (1982). Rate of environmental change and adaptation in the copepod *Eurytemora affinis*. Evolution *36*, 298–306.
48. Karlsson, K., Puiac, S., and Winder, M. (2018). Life-history responses to changing temperature and salinity of the Baltic Sea copepod *Eurytemora affinis*. Mar. Biol. *165*, 30. https://doi.org/10.1007/s00227-017-3279-6.
49. Stern, D.B., Anderson, N.W., Diaz, J.A., and Lee, C.E. (2022). Genome-wide signatures of synergistic epistasis during parallel adaptation in a Baltic Sea copepod. Nat. Commun. *13*, 4024. https://doi.org/10.1038/s41467-022-31622-8.
50. Park, T.S. (Ph.D. Thesis, University of Washington. 1965). The Biology of a Calanoid Copepod *Epilabidocera amphitrites* McMurrich.
51. Gerber, L., Lee, C.E., Grousset, E., Blondeau-Bidet, E., Boucheker, N.B., Lorin-Nebel, C., Charmantier-Daures, M., and Charmantier, G. (2016). The legs have it: *In situ* expression of ion transporters V-type H^+-ATPase and Na^+/K^+-ATPase in the osmoregulatory leg organs of the invading copepod *Eurytemora affinis*. Physiol. Biochem. Zool. *89*, 233–250. https://doi.org/10.1086/686323.
52. Johnson, K.E., Perreau, L., Charmantier, G., Charmantier-Daures, M., and Lee, C.E. (2014). Without gills: Localization of osmoregulatory function in the copepod *Eurytemora affinis*. Physiol. Biochem. Zool. *87*, 310–324. https://doi.org/10.1086/674319.
53. Stern, D.B., and Lee, C.E. (2020). Evolutionary origins of genomic adaptations in an invasive copepod. Nat. Ecol. Evol. *4*, 1084–1094. https://doi.org/10.1038/s41559-020-1201-y.
54. Lee, C.E. (2021). Ion transporter gene families as physiological targets of natural selection during salinity transitions in a copepod. Physiology *36*, 335–349. https://doi.org/10.1152/physiol.00009.2021.
55. Posavi, M., Gulisija, D., Munro, J.B., Silva, J.C., and Lee, C.E. (2020). Rapid evolution of genome-wide gene expression and plasticity during saline to freshwater invasions by the copepod *Eurytemora affinis* species complex. Mol. Ecol. *29*, 4835–4856. https://doi.org/10.1111/mec.15681.
56. Lee, C.E., Kiergaard, M., Gelembiuk, G.W., Eads, B.D., and Posavi, M. (2011). Pumping ions: Rapid parallel evolution of ionic regulation following habitat invasions. Evolution *65*, 2229–2244. https://doi.org/10.1111/j.1558-5646.2011.01308.x.
57. Diaz, J., Stern, D., and Lee, C.E. (2023). Local adaptation despite gene flow in copepod populations across salinity and temperature gradients in the Baltic and North Seas. Authorea Preprints. https://doi.org/10.22541/au.168311545.58858033/v1.
58. Engel, R.A. (1962). *Eurytemora affinis*, a calanoid copepod new to Lake Erie. Ohio J. Sci. *62*, 252.
59. Merilä, J., and Hendry, A.P. (2014). Climate change, adaptation, and phenotypic plasticity: The problem and the evidence. Evol. Appl. *7*, 1–14. https://doi.org/10.1111/eva.12137.

60. Clausen, J., Keck, D.D., and Hiesey, W.M. (1947). Heredity of geographically and ecologically isolated races. Am. Nat. *81*, 114–133. https://doi.org/10.1086/281507.
61. Gicklhorn, J. (1931). Elektive vitalfärbungen im dienste der anatomie und physiologie der exkretionsorgane von wirbellosen (Cladoceren als Beispiel). Protoplasma *13*, 701–724. https://doi.org/10.1007/BF01599659.
62. Binns, R. (1969). The physiology of the antennal gland of *Carcinus maenas* (L.). J. Exp. Biol. *51*, 41–45. https://doi.org/10.1242/jeb.51.1.41.
63. Riegel, J.A., and Kirschner, L.B. (1960). The excretion of inulin and glucose by the crayfish antennal gland. Biol. Bull. *118*, 296–307.
64. Lin, S.C., Liou, C.H., and Cheng, J.H. (2000). The role of the antennal glands in ion and body volume regulation of cannulated *Penaeus monodon* reared in various salinity conditions. Comp. Biochem. Physiol. Mol. Integr. Physiol. *127*, 121–129. https://doi.org/10.1016/S1095-6433(00)00245-2.
65. Khalifi, K., Salamat, N., and Movahedinia, A. (2021). Microanatomy of the antennal glands and their Na^+/K^+-ATPase activity in three true crab species (Brachyura), *Portunus pelagicus* (Linnaeus, 1758) (Portunidae), *Macrophthalmus dentipes* Lucas in Guérin, 1836 (Macrophthalmidae) and *Eriocheir hepuensis* Dai, 1991 (Varunidae). Crustaceana *94*, 1359–1376. https://doi.org/10.1163/15685403-bja10159.
66. Tyson, G.E. (1969). The fine structure of the maxillary gland of the brine shrimp, *Artemia salina*: The efferent duct. Z. Zellforsch. Mikrosk. Anat. *93*, 151–163. https://doi.org/10.1007/BF00336687.
67. Peterson, D.R., and Loizzi, R.F. (1974). Biochemical and cytochemical investigations of (Na^+-K^+)-ATPase in the crayfish kidney. Comp. Biochem. Physiol. A Comp. Physiol. *49*, 763–773.
68. Lee, C.E., and Gelembiuk, G.W. (2008). Evolutionary origins of invasive populations. Evol. Appl. *1*, 427–448. https://doi.org/10.1111/j.1752-4571.2008.00039.x.
69. Alekseev, V.R., and Souissi, A. (2011). A new species within the *Eurytemora affinis* complex (Copepoda: Calanoida) from the Atlantic Coast of USA, with observations on eight morphologically different European populations. Zootaxa *2767*, 41–56. https://doi.org/10.11646/zootaxa.2767.1.4.
70. Lee, C.E. (2000). Global phylogeography of a cryptic copepod species complex and reproductive isolation between genetically proximate "populations". Evolution *54*, 2014–2027. https://doi.org/10.1111/j.0014-3820.2000.tb01245.x.
71. McDonough, A.A., Veiras, L.C., Minas, J.N., and Ralph, D.L. (2015). Considerations when quantitating protein abundance by immunoblot. Am. J. Physiol. Cell Physiol. *308*, C426–C433. https://doi.org/10.1152/ajpcell.00400.2014.
72. Cao, Q., Blondeau-Bidet, E., and Lorin-Nebel, C. (2022). Intestinal osmoregulatory mechanisms differ in Mediterranean and Atlantic European sea bass: A focus on hypersalinity. Sci. Total Environ. *804*, 150208. https://doi.org/10.1016/j.scitotenv.2021.150208.
73. IPBES (2019): Global assessment report on biodiversity and ecosystem services of the Intergovernmental Science-Policy Platform on Biodiversity and Ecosystem Services. E. S. Brondizio, J. Settele, S. Díaz, and H. T. Ngo (editors). IPBES secretariat, Bonn, Germany. 1148 pages. https://doi.org/10.5281/zenodo.3831673
74. Jude, D.J., Reider, R.H., and Smith, G.R. (1992). Establishment of Gobiidae in the Great Lakes basin. Can. J. Fish. Aquat. Sci. *49*, 416–421. https://doi.org/10.1139/f92-047.
75. Martel, A.L., and Madill, J.B. (2018). Twenty-six years (1990–2015) of monitoring annual recruitment of the invasive zebra mussel (*Dreissena polymorpha*) in the Rideau River, a small river system in Eastern Ontario, Canada. Can. J. Zool. *96*, 1071–1079. https://doi.org/10.1139/cjz-2017-0360.
76. Brown, J., Whiteley, N.M., Bailey, A.M., Graham, H., Hop, H., and Rastrick, S.P.S. (2020). Contrasting responses to salinity and future ocean acidification in arctic populations of the amphipod *Gammarus setosus*. Mar. Environ. Res. *162*, 105176. https://doi.org/10.1016/j.marenvres.2020.105176.
77. Lucu, Č., and Towle, D.W. (2003). Na^+/K^+-ATPase in gills of aquatic crustacea. Comp. Biochem. Physiol. Mol. Integr. Physiol. *135*, 195–214. https://doi.org/10.1016/S1095-6433(03)00064-3.
78. Souissi, A., Hwang, J.S., and Souissi, S. (2021). Reproductive trade-offs of the estuarine copepod *Eurytemora affinis* under different thermal and haline regimes. Sci. Rep. *11*, 20139. https://doi.org/10.1038/s41598-021-99703-0.
79. Souissi, S., and Souissi, A. (2021). Promotion of the development of sentinel species in the water column: Example using body size and fecundity of the egg-bearing calanoid copepod *Eurytemora affinis*. Water (Switzerland) *13*, 1442. https://doi.org/10.3390/w13111442.
80. Kuismanen, L., Forsblom, L., Engström-Öst, J., Båmstedt, U., and Glippa, O. (2020). Salinity effects on egg production, hatching, and survival of *Eurytemora affinis* (Copepoda, Calanoida). Crustaceana *93*, 429–445. https://doi.org/10.1163/15685403-00003988.
81. Waddington, C.H. (1953). Genetic assimilation of an acquired character. Evolution *7*, 118–126.
82. Lande, R. (2009). Adaptation to an extraordinary environment by evolution of phenotypic plasticity and genetic assimilation. J. Evol. Biol. *22*, 1435–1446. https://doi.org/10.1111/j.1420-9101.2009.01754.x.
83. Chevin, L.M., and Lande, R. (2010). When do adaptive plasticity and genetic evolution prevent extinction of a density-regulated population? Evolution *64*, 1143–1150. https://doi.org/10.1111/j.1558-5646.2009.00875.x.
84. Scheiner, S.M., Barfield, M., and Holt, R.D. (2020). The genetics of phenotypic plasticity. XVII. Response to climate change. Evol. Appl. *13*, 388–399. https://doi.org/10.1111/eva.12876.
85. DeWitt, T.J., Sih, A., and Wilson, D.S. (1998). Costs and limits of phenotypic plasticity. Trends Ecol. Evol. *13*, 77–81.
86. Lee, C.E., Remfert, J.L., and Gelembiuk, G.W. (2003). Evolution of physiological tolerance and performance during freshwater invasions. Integr. Comp. Biol. *43*, 439–449.
87. Lee, C.E., Remfert, J.L., and Chang, Y.M. (2007). Response to selection and evolvability of invasive populations. Genetica *129*, 179–192. https://doi.org/10.1007/s10709-006-9013-9.
88. Towle, D.W. (1984). Membrane-bound ATPases in arthropod ion-transporting tissues. Am. Zool. *24*, 177–185. https://doi.org/10.1093/icb/24.1.177.
89. Lin, H., and Randall, D. (1991). Evidence for the presence of an electrogenic proton pump on the trout gill epithelium. J. Exp. Biol. *161*, 119–134. https://doi.org/10.1242/jeb.161.1.119.
90. Clausen, M.V., Hilbers, F., and Poulsen, H. (2017). The structure and function of the Na,K-ATPase isoforms in health and disease. Front. Physiol. *8*, 371. https://doi.org/10.3389/fphys.2017.00371.
91. Whiteley, N.M., Scott, J.L., Breeze, S.J., and McCann, L. (2001). Effects of water salinity on acid-base balance in decapod crustaceans. J. Exp. Biol. *204*, 1003–1011.
92. Kültz, D., Fiol, D., Valkova, N., Gomez-Jimenez, S., Chan, S.Y., and Lee, J. (2007). Functional genomics and proteomics of the cellular osmotic stress response in "non-model" organisms. J. Exp. Biol. *210*, 1593–1601. https://doi.org/10.1242/jeb.000141.
93. Du, Z., Gelembiuk, G., Moss, W., Tritt, A., and Lee, C.E. (2023). The genome architecture of a copepod invading novel habitats. ResearchSquare. https://doi.org/10.21203/rs.3.rs-3002580/v3.
94. Schindelin, J., Arganda-Carreras, I., Frise, E., Kaynig, V., Longair, M., Pietzsch, T., Preibisch, S., Rueden, C., Saalfeld, S., Schmid, B., et al. (2012). Fiji: An open-source platform for biological-image analysis. Nat. Methods *9*, 676–682. https://doi.org/10.1038/nmeth.2019.
95. Jones, M.V., and Calabresi, P.A. (2007). Agar-gelatin for embedding tissues prior to paraffin processing. Biotechniques *42*, 569–570. https://doi.org/10.2144/000112456.
96. Ohgane, K., and Yoshioka, H. (2019). Quantification of gel bands by an Image J macro, band/peak quantification tool v1. protocols.io. https://doi.org/10.17504/protocols.io.7vghn3w.
97. Kapur, J.N., Sahoo, P.K., and Wond, A.K. (1985). A new method for grey-level picture thresholding using the entropy of the histogram. Comput. Vis. Graph Image Process *29*, 223–237. https://doi.org/10.1016/0165-1684(80)90020-1.
98. R Core Team (2020). R: A Language and Environment for Statistical Computing (R Foundation for Statistical Computing).

STAR★METHODS

KEY RESOURCES TABLE

REAGENT or RESOURCE	SOURCE	IDENTIFIER
Antibodies		
Mouse monoclonal anti-Na^+-K^+-ATPase α-subunit (α5)	DSHB	Cat# A-11001; RRID: AB_2166869
IRDye® 800CW Donkey anti-mouse IgG	Li-COR	RRID:AB_621847
Goat anti-mouse; Alexa Fluor 488 nm	Invitrogen	RRID: AB_2534069
Chemicals, peptides, and recombinant proteins		
protease inhibitors	Thermo Scientific	Cat# 87785
loading buffer	Li-COR	Cat# 928-40004
Chameleon® Duo protein size marker	Li-COR	Cat# 928-60000
Experimental models: Organisms/strains		
Eurytemora carolleeae, Racine Harbor (Lake Michigan), Wisconsin, USA	The Lee Laboratory	RacineB
Eurytemora carolleeae, Baie de L'Isle Verte (St. Lawrence estuary), Quebec, Canada	The Lee Laboratory	LV20
Software and algorithms		
Image Studio Lite v5.2.5	LI-COR Biosciences	RRID:SCR_013715
FIJI (ImageJ) v2.3.0/1.53q	ImageJ	RRID:SCR_002285
Fiji macro "_BandPeakQuantification.ijm"	Ohgane, K., and Yoshioka, H. (2019)	https://doi.org/10.17504/protocols.io.7vghn3w
R v4.3.0	The R Foundation	RRID:SCR_001905
Other		
Mini-PROTEAN TGX Precast Gel	Bio-Rad	Cat# 4561085

RESOURCE AVAILABILITY

Lead contact

Further information and requests for resources and reagents should be directed to and will be fulfilled by the lead contact Catherine Lorin-Nebel (catherine.lorin@umontpellier.fr).

Materials availability

This study did not generate new unique reagents.

Data and code availability

- All data reported in the paper will be shared by the lead contact upon request.
- This paper does not report any original code.
- Any additional information required to reanalyze the data reported in this paper is available from the lead contact upon request.

EXPERIMENTAL MODEL AND STUDY PARTICIPANT DETAILS

Population sampling

Population sampling was performed in 2020 for adult males and females of both the saline and freshwater populations of *Eurytemora carolleeae*[69] (Atlantic clade of the *Eurytemora affinis* complex). The saline population was sampled in October of 2020 from a tidal marsh along the St. Lawrence Seaway, in Baie de L'isle Verte, Quebec, Canada (48°00′14″ N, 69°25′31″ W), where salinity fluctuates seasonally between 5 and 40 PSU. Samples from a freshwater population were collected in summer of 2020 from Lake Michigan at Racine Harbor, Wisconsin, USA (42°43′46″N, 87°46′44″W), where salinity is stable at 0 PSU (conductivity of 300 μS/cm). Both saline and freshwater populations were maintained in the lab for two years (approximately 24 generations) at their native salinities (15 and 0 PSU respectively) prior to the experiment. Saline populations were fed the saltwater alga *Rhodomonas salina*, whereas freshwater populations were fed the freshwater alga *Rhodomonas minuta*.

METHOD DETAILS

Common garden experimental design

To distinguish between acclimatory versus evolutionary shifts in NKA immunolocalization and expression, saline and freshwater populations of *E. carolleeae* were reared under common garden conditions. At the start of this experiment, ovigerous females from the saline population (St. Lawrence estuary, Canada) and freshwater population (Lake Michigan, Wisconsin) were transferred to a common salinity of 5 PSU ($N = 30$ per population). Once nauplii (larvae) hatched, the adult mothers were removed from the beakers and the nauplii (larvae) were reared under this common salinity (5 PSU) until metamorphosing to the copepodid (juvenile) stage. Groups of juveniles were then gradually transferred (4-day salinity decline: 5 PSU, 2.5 PSU, 1 PSU, 0 PSU; 4-day salinity increase: 5 PSU, 8 PSU, 10 PSU, 15 PSU) to the treatment salinities of 0 (Lake Michigan water), 5, and 15 PSU. Approximately 200 juveniles were transferred to each salinity treatment. The populations were not reared at the treatment salinities for more than one generation to avoid imposing natural selection on the larval stages (nauplii). Previous studies have shown that 0 and 15 PSU induce high mortality and impose strong selection on the larval stages that are not native to those salinities.[86,87] In addition, a prior study showed that maternal environmental effects (effects of maternal rearing salinity on survival or performance of offspring) have minimal effects on ion transporter enzyme activity levels.[56] After one week of exposure to the treatment salinities as adults, the copepods were preserved for Western blot and immunohistochemical analyses.

Whole-animal Western Blot immunostaining of NKA

To determine the amount of NKA protein in whole copepods, Western blot band intensity quantification was conducted. Animals from each common garden treatment were frozen in SEI buffer (0.3 mol L^{-1} sucrose, 0.1 mol L^{-1} imidazole; 0.02 mol L^{-1} EDTA; pH 7.4) containing protease inhibitors (Thermo Scientific, ref. 87785) and stored at −20°C until analysis. Six animals from each treatment were thawed and photographed using a Leitz Laborlux microscope equipped with a Leica DC300F digital camera. Body size (i.e., prosome length in μm) measurements were taken from the top of the head to the end of the prosome using Fiji image analysis software package (2.3.0/1.53q)[94](Figure 3). These animals were then transferred directly to loading buffer (Li-COR, ref. 928–40004) with β-mercaptoethanol and then homogenized using a potter-type mortar and pestle (Bel-Art Disposable Pestles, Ref: F199230001). For an internal control a "super-mix" sample was also homogenized which contained 300 copepods from a combination of the treatments. This super-mix served as calibrator to normalize variation between electrophoresis gels.[71,72]

The homogenized animals were incubated on ice for 30 min and then loaded into Mini-PROTEAN TGX Precast Gel (Bio-Rad, ref. 4561085) for electrophoresis. Each gel included each treatment from both populations in order to compare all treatments on a single membrane and a super-mix sample. Each gel also contained a protein size marker (Chameleon Duo, Li-COR, ref. 928–60000) and a 10-μg standard (purified protein extract from 500 copepods) to control for variation among gels. After electrophoretic migration, proteins were transferred onto a 0.2 μm PVDF membrane (Bio-Rad, Ref: LC2000) using a Trans-Blot Turbo Transfer system (Bio-Rad, ref. 1704150). Blots were blocked with a blocking buffer (BSA 3% + 0.2% and Tween 20) for 1 h at room temperature with gentle agitation. The membrane was then exposed to a primary antibody that targets the ion transporter protein NKA alpha subunit (mouse monoclonal anti-Na^+/K^+-ATPase α-subunit (α5), Developmental Studies Hybridoma Bank, maintained at the University of Iowa, Department of Biology, Iowa City, IA, USA). The primary antibody was diluted to 0.042 μg/mL in blocking buffer (BSA 3% + 0.2% and Tween 20) and placed overnight at 4°C with gentle agitation. The membranes were then rinsed and exposed to secondary antibodies (IRDye 800CW Donkey anti-mouse IgG, Li-COR ref. 926–32212) applied at 0.5 μg/mL diluted in blocking buffer (BSA 3% + 0.2% Tween 20 + SDS 10%) and then rinsed again before imaging. Membranes were imaged with Image Studio Lite (RRID:SCR_013715) (software application) using an exposure of 1.5 min.

Immunostaining of NKA whole mounts (*in toto*)

To observe which specific organs and tissues were expressing NKA in the whole animal, *in toto* immunostaining was conducted. Common garden animals were preserved in Paraformaldehyde (PFA) (4%) fixative for 24 h at 4°C and rinsed 3 times in PBS. The PFA samples were then stored in methanol at −20°C until use for histological analysis. For analysis, animals from each treatment were rehydrated in a series of ethanol baths (70% and 50%) and then rinsed in PBS. Sonication was performed using several short pulses (2 pulses, 3 s each) in a bath ultrasonicator to facilitate penetration of antibodies. Animals were washed several times in 0.1M PBT (0.3% Trition X- 100, 1.5% DMSO, 0.5% BSA in PBS pH 7.3), and then incubated in a bath of PBT +5% natural goat serum (NGS 5%). The same NKA primary antibody described above was diluted to 12 μg/mL in PBT + NGS 5% and the animals were bathed in this mixture for 3 days at 4°C, with extensive rinsing in PBT after incubation. A secondary antibody (goat anti-mouse; Invitrogen, Ref: A11001, tagged with the fluorochrome AF 488 nm) was applied to the animals at 0.2 μg/mL in PBT + NGS 5% overnight at 4°C, again with extensive rinsing post incubation. The nuclei of the samples were stained with 4′, 6-diamidino-2-phenylindole (DAPI) at 1 μg/mL for 40 min and then rinsed. Specimens were mounted on slides with Slow FadeTM Diamond Antifade mounting liquid (refractive index: 1.42; Invitrogen). A drop of Dow Corning grease was added to each corner of the slide to create a barrier that prevents the coverslip from crushing the specimen during microscopy.

Specimens used in *in toto* immunostaining were viewed in 3D on a confocal microscope (Confocal ZEISS LSM880 FastAiryscan, MRI platform).

Immunostaining of maxillary glands with NKA (*in situ*)

In situ quantification of NKA expression was conducted on sagittally sliced individuals, so that the cells and structure within both maxillary glands on each animal could be observed. From the PFA preserved common garden animals (see previous section), 6 individuals from each salinity treatment for each population (n = 36) were photographed and their body size (i.e., prosome length) (μm) was measured using the same method described in the Western blot section (see above). These same copepods were then stained with eosin and individually embedded in agarose (2%) and gelatin (2.5%) in MilliQ water,[95] allowing lateral orientation of copepods before paraffin slicing. Meticulous attention was made to conserve all portions of the animal throughout the entire slicing process. Samples were then fully dehydrated in a series of ethanol baths (95% and 100%), immersed in Diasolv and paraffin baths, and then embedded in paraffin wax at 58°C. The paraffin blocks were cut into 5 μm thick ribbons in succession on a Leica RM2255 microtome and mounted on superfrost slides (SuperFrost Plus, Menzel Gläser) and then dried at 37°C for at least one night.

For immunostaining, the slides were dewaxed through a series of Diasolv, butanol, and descending ethanol baths (100%, 90%, 70%, and 50%) and finally rinsed in PBS. Slides were next incubated in 10 mM sodium citrate buffer and microwaved (at 80% power twice for 1 min 30 s) to reveal the antigenic sites. After cooling at room temperature, the slides were immersed for 10 min in a 10 mM PBS solution with 0.02% Tween 20 and 150 mM NaCl (pH 7.3). Saturation to block nonspecific antigenic sites was performed in a solution of BSA 3% in PBS at room temperature for 20 min. The slides were then rinsed in three PBS baths and then incubated overnight at 4°C with 12 μg/mL of NKA primary antibodies diluted in PBS-BSA 0.3%. Control slides were also exposed to the same conditions, but without the primary antibody. Finally, all slides, including the controls, were exposed to the same secondary antibody used for whole mounts diluted to 0.2 μg/mL in PBS-BSA 0.3%. All slides were incubated for 6 min with DAPI at 1 μg/mL and then rinsed in PBS. The slides were mounted with the aqueous-based mounting medium used above and stored at 4°C in the dark until observed.

All cut specimens were photographed with a fluorescence microscope (Leica Thunder, platform MRI, Montpellier) using GFP and DAPI filters, along with brightfield images. Every section was carefully examined, and those containing maxillary gland tissue were identified (with two maxillary glands per individual). These identified sections were then uniformly photographed using the same magnification, fluorochrome exposure time, and light intensity, based on predetermined settings to detect fluorescence at each salinity treatment while avoiding overexposure.

QUANTIFICATION AND STATISTICAL ANALYSIS

Whole animal quantification of Western Blot NKA band signal intensity

Whole animal NKA band intensity from Western Blot images was quantified using Fiji. The macro "_BandPeakQuantification.ijm" was used to determine band's signal intensity calculated as the integrated intensity minus background noise.[96]

The NKA band signal intensity for each loaded sample was standardized by dividing fluorescent intensity (integrated pixel intensity) by the sum of the prosome length (μm) of the six individual copepods loaded onto the electrophoresis gel. Variation among membranes was also controlled for by dividing band signals on a membrane by the super-mix band intensity (integrated pixel intensity) on the corresponding membrane. Thus, this normalized Western blot band signal intensity reflects a measure of the response variable *Whole-Animal NKA*.

In situ quantification of NKA expression area and fluorescence intensity in the maxillary glands

The area and intensity of NKA expression in the maxillary glands were quantified for each cut containing maxillary glands using Fiji. Each image was observed using uniform upper and lower pixel intensity thresholds, along with RenyiEntropy auto thresholding algorithms.[97] This thresholding was performed to remove background fluorescence and autofluorescence in the same manner for each image. Once an image went through thresholding, measurements were taken for (1) total fluorescent area (μm^2) and (2) fluorescence intensity (pixel intensity units) of NKA expression (mean, minimum, and maximum values) for each cut with an immunolabeled maxillary gland (IMG).

Values for response variables *NKA IMG Area, NKA IMG Intensity,* and *Amount of NKA* were obtained in the following manner. (1) *NKA IMG Area* (μm^2) was determined to reflect the abundance of ion transporting epithelia with NKA expression in the maxillary glands. First, the total volume (μm^3) of NKA immunolabeling in the maxillary glands (volume of maxillary glands with immunolabeling) was calculated by summing the fluorescent area (μm^2) on each cut within an individual copepod and multiplying this area by 5 μm (as each cut was 5 μm thick). This measure of total volume was then standardized by dividing the value by the individual's prosome length (μm) (i.e., body size), yielding the response variable *NKA IMG Area* (μm^2). (2) *NKA IMG Intensity* (pixel value) in the maxillary glands was determined by calculating the average pixel intensity corresponding to the maximum florescence intensity on each cut within an individual. This value thus reflects the mean of the brightest points on each cut within an individual's maxillary glands. (3) *Amount of NKA* in the maxillary glands was calculated by multiplying *NKA IMG Area* and *NKA IMG Intensity*. Standard deviation was propagated for the product of the two variables (*NKA IMG Area* and *NKA IMG Intensity*) and calculated as:

$$\frac{\sigma_x}{\mu_x} = \sqrt{\left(\frac{\sigma_a}{\mu_a}\right)^2 + \left(\frac{\sigma_b}{\mu_b}\right)^2}$$

where σ = standard deviation, μ = mean, subscripts x = *Amount of NKA*, a = *NKA IMG Area*, and b = *NKA IMG Intensity*.

Statistical analyses

All analyses were performed using the statistical software package R (version 4.3.0).[98] All data were tested for normality using a Shapiro-Wilk normality test and transformed if normality standards were not met. If data could not be normalized, non-parametric tests were used (Tables 2, S1, and S2). We examined the effects of the factors *Population* (saline versus freshwater populations), *Salinity* (0, 5, 15 PSU), and *Population* × *Salinity* interaction on the response variables *Body Size*, *Whole-Animal NKA*, *NKA IMG Area*, and *Amount of NKA* using a Two-way Analysis of Variance (two-way ANOVA). For the response variable *NKA IMG Intensity*, a nonparametric Kruskal-Wallis test was used to examine the effects of *Population*, *Salinity*, and *Population x Salinity* because the data were negatively skewed.

All factors were treated as fixed effects. When the effects of factors were significant using ANOVA, *post hoc* pairwise Tukey comparisons were performed. In addition, to test the *a priori* hypothesis that population level differences exist at each treatment salinity, comparisons between populations at each salinity were made for all response variables using the Student's t test. To examine differences in NKA staining between treatment salinities, *a priori* comparisons were made for each population using Student's t-tests. To measure the effect size between significant comparisons, the strictly standardized mean difference *(β)* was calculated as:

$$\beta = \frac{\mu_1 - \mu_2}{\sqrt{\sigma_1^2+\sigma_2^2}},$$

where μ = mean of treatment salinity or populations being compared, σ = standard deviation of the mean.

To examine the level of variance in *Amount of NKA* staining among treatment salinities, the coefficient of variation was calculated for each population. We determined the covariance between *NKA IMG Area* and *NKA IMG Intensity* by calculating the Pearson's correlation coefficient. For the response variable *NKA IMG Intensity*, an *a priori* Wilcoxon rank-sum test was used to compare population level differences at each treatment salinity and differences between salinities within each population.